MEASUREMENTS OF SOURCE STRENGTHS AT 29·9 MHz

By E. A. Finlay* and B. B. Jones*

[Manuscript received 24 October 1972]

Abstract

A survey of the region of sky between declinations $-4°$ and $-64°$ has been completed at a frequency of 29·9 MHz at the Fleurs Radio Observatory of the School of Electrical Engineering, University of Sydney. Aperture synthesis has been used to form a beam of $0°\cdot 8$ diameter. The flux densities of 175 sources have been measured and referred to absolute measurements of certain strong sources. Most of the source fluxes are consistent with an extrapolation of the power law spectra determined from high frequency measurements but a few show significant deviations. Absorption by the interstellar medium of sources at low galactic latitudes has only been observed for $|b| < 3°$ and appears to be negligible at higher latitudes.

I. Introduction

Very little work has been published on the strengths of southern radio sources at frequencies below 80 MHz and, since the galactic survey at 19·7 MHz by Shain *et al.* (1961), no high resolution low-frequency observations of the southern sky have been published. The aperture synthesis telescope of the Fleurs Radio Observatory of the School of Electrical Engineering, University of Sydney, was constructed to help fill this gap (Finlay and Jones 1972). The instrument has a beamwidth of $0°\cdot 8$ and an operating frequency of 29·9 MHz. The choice of frequency appears to have been fortunate since at 29·9 MHz long spells of interference-free observing occur quite frequently. At lower frequencies the problem of interference reflected from the ionosphere becomes rapidly more severe and was a serious limitation on observation at 19·7 MHz.

II. Instrument

The telescope consists of a long east–west (EW) array together with two small portable arrays which are placed symmetrically to the north and south of the EW array at various spacings. The EW aerial consists of a collinear array of half-wave elements 106λ long ($\sim$ 1 km) fed in phase to form a fan beam along the meridian. The elements are fed in groups of six from a balun between the two central elements of the group. The other elements of the group are separated by phase reversing coils. The signal from each group is coupled into a continuous coaxial feedline through a directional coupler with coupling chosen to give a grading of $1+\frac{2}{3}\cos(\pi x/L)$ to the array, where x is the distance from the centre of the array and $2L$ is the total length of the array. The half-wave elements are at a height above ground of nearly $\frac{1}{2}\lambda$ and so, to avoid a dip in the response near the zenith, directors at a height of $0\cdot 1\,\lambda$ above the driven elements are used.

* School of Electrical Engineering, University of Sydney, Sydney, N.S.W. 2006.

Each small portable array consists of three parallel half-wave dipoles spaced $0 \cdot 5\lambda$ apart in the north–south direction. The dipoles are mounted $0 \cdot 1\lambda$ above a wire-mesh ground plane, which rests directly on the ground so as to provide a continuation of the ground plane. The patterns of the north–south (NS) and EW arrays are shown in Figure 1.

The outputs from the three antennas are returned to a central receiver hut. There the signals from the north and south arrays are combined in a hybrid to form their sum and difference, and the three signals $N+S$, $N-S$, and EW are amplified over a bandwidth of 200 kHz. The in-phase correlation of $N+S$ with EW and the quadrature correlation of $N-S$ with EW are formed by multiplier type correlators. These correlations are the cosine and sine outputs required for aperture synthesis.

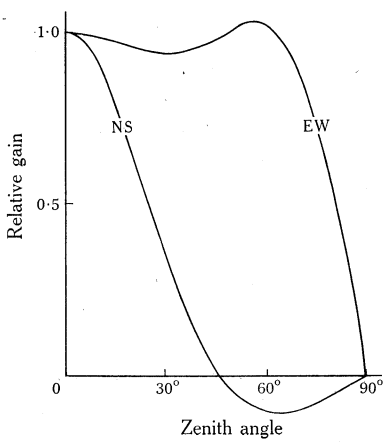

Fig. 1.—Calculated north–south field patterns of the north–south (NS) and east–west (EW) arrays.

For the present observations, the cosine and sine outputs were recorded in analogue form on paper charts with a time constant of 1 s. They were later digitized by hand, by means of a D-MAC chart to paper-tape converter, with a time constant of $\sim$ 1 min. This procedure enabled interference and scintillation spikes to be removed and allowed portions of the records, where interference appeared to make them unreliable, to be discarded.

The grid of spacings for the NS aerial was nonuniform, so that about half the grading necessary to keep sidelobes down to an acceptable level was provided by a density taper, the remainder being provided as amplitude taper. The spacing between positions ranged from $0 \cdot 76$ to $1 \cdot 76\lambda$, with 50 spacings being used in all. As well as increasing the sensitivity, this made the grating response appear as a series of low ripples rather than as a replica of the main response, which would occur for a uniform grid of spacings. These low ripples are more easily recognized as being spurious.

The set of 50 outputs for each minute of sidereal time was processed by computer to form the Fourier transform which, after correction for the beam shape of the individual aerials, gave the brightness distribution along the strip of sky contained in the fan beam of the EW array. The resulting synthesized beam had a width of about $0° \cdot 8$ in right ascension and $0° \cdot 8 \sec(\delta + 33° \cdot 86)$ in declination at declination δ. The synthesis was performed over a field of 30° either side of the zenith (declination $-33° \cdot 86$). The list of sources was prepared by finding the peak fluxes from computer-drawn contour maps of the synthesized sky brightness.

III. Absolute Flux Scale

Since so few measurements have been made on southern hemisphere sources at low frequencies, there has not been established a reliable set of low-frequency flux calibrators. The region of overlap (declination $-4°$ to $-10°$) of the present survey and the Cambridge 38 MHz survey (Williams *et al.* 1966) is too small to allow a satisfactory comparison and, in any case, the Cambridge observations in this region were made with a fan beam and may be in considerable error due to confusion. In view of this it was considered necessary to measure absolutely the fluxes of a number of sources.

The absolute measurements were made by a method similar to that described by Little (1958) and Wyllie (1969*a*). The power output from the EW aerial and the correlated output of an interferometer consisting of a small aerial of calculable gain and the EW aerial were measured simultaneously. Both the in-phase and quadrature components of the correlation between the two aerials were measured. For these measurements one of the portable aerials used for the survey was rearranged so that the three dipoles were collinear in order to obtain a broader north–south pattern, thereby permitting the measurement of some more northerly sources covered by the northern hemisphere surveys. The gain of this aerial configuration can readily be calculated on the assumption that the ground acts as a continuation of the wire-mesh ground plane. The wire-mesh ground plane for each dipole measures $0\cdot5\lambda\times0\cdot75\lambda$ and the impedance of the dipole has been found to change by less than $0\cdot1\%$ if the ground plane is extended.

Table 1

Absolute measurements of source strengths at 29·9 MHz

Source		No. of measurements	$S_{29.9}$ (f.u.)	$\Delta S_{29.9}$ (f.u.)	$S_{29.9}/S_{\mathrm{KPW}}$*
Taurus A	3C 144	7	2610	95	1·00
Hydra A	3C 218	5	1512	81	1·07
Virgo A	3C 274	6	4560	300	1·04
13S6A	1343−60	4	1660	190	—
16S6A	1610−60	7	3280	230	—
Hercules A	3C 348	4	2380	250	1·11

* S_{KPW} are 29·9 MHz flux densities obtained by extrapolation from the source spectra quoted by Kellermann *et al.* (1969).

Throughout the measurements, the system gain was periodically checked by replacing both aerials by noise diodes, to which the aerials had been matched, and which were themselves calibrated against thermal loads. The gains of the correlators were monitored by injecting a known amount of correlated noise power into each aerial line through directional couplers.

The calculation of source strengths from these measurements required small corrections for the loss of coherence of the signals over the receiver passbands. In no case did this correction exceed 8%. The correction took into account the distributed nature of the EW aerial and the shape of the receiver passband as well as the difference in cable lengths to the aerials.

The flux densities of six sources determined by this method are given in Table 1. The chief source of error in these values is confusion of the EW power record, but the error estimates given in the table include also the effects of noise on the records and possible errors in the calibration. In the case of 3C sources, the ratios of the measured fluxes to those predicted from the spectra quoted by Kellermann *et al.* (1969) are included in the table. The weighted average of these ratios, 1·04, may be taken as the ratio of the present flux scale to that of Kellermann *et al.* (1969). This latter scale agrees with the scale established earlier by Conway *et al.* (1963) at low frequencies.

IV. Source Strengths Measured from Synthesis Maps

(*a*) *Sensitivity*

At 29·9 MHz the system temperature is determined almost entirely by the sky temperature, the receiver noise being insignificant in comparison. The sky temperature, averaged over the antenna beam, ranges from $\sim$ 15000 K at $04^{h}00^{m}$ to $\sim$ 85000 K at $18^{h}00^{m}$, so that there is a large variation in sensitivity over the region being mapped. For the coldest part of the sky the r.m.s. fluctuation is about 5 f.u. on the synthesized maps. Towards the edges of the narrower north–south patterns of the small aerials, the signal to noise ratio is reduced by a factor of about three.

(*b*) *Observing Conditions*

Only records that were substantially free from obvious interference and ionospheric scintillations were used for the survey. This required that observations be made several times at each spacing until a complete 24 hr record at that spacing could be compiled from the various observations. An idea of the consistency of the records may be gained from an examination of Figure 2, in which the cosine and sine components for the source Hydra A are plotted for selected groups of consecutive spacings. The phases have been rotated numerically so that the sine output would be zero in the absence of refraction. It appears that the rejection of records which showed visible ionospheric effects (scintillation and ionospheric propagated interference) has resulted in the retention only of those in which refraction was small compared with the synthesized beamwidth; otherwise the sine components would be large for some spacings.

The most noticeable features are that the amplitudes at some spacings are reduced and, at the more distant spacings, phase shifts are becoming significant. These must be ionospheric effects since the aerial phases and temperatures were checked regularly. These effects produce spurious irregular responses extending north–south at the right ascensions of strong sources, thereby reducing the reliability of the map near the right ascension of any source stronger than about 500 f.u. This variation in sensitivity and reliability over the map means that the list of sources cannot be regarded as complete above a certain limiting flux value, but rather as a list of all those sources for which reliable flux density measurements could be made.

(*c*) *Gain as Function of Zenith Angle*

The north–south envelope of the interferometer lobes is determined mainly by the small movable arrays. As the geometry and current distribution of these arrays is well known, their north–south patterns can be calculated accurately. The current distribution in elements of the EW array is less accurately known but since its north–south pattern is much broader it is less important. The relative deflections on the EW power records for the sources listed in Table 1 were consistent with the EW pattern

(Fig. 1) calculated from the design current distribution. The response near the zenith was checked by comparing the integrated flux density of Fornax A ($\delta = -37°$) obtained from the EW power record with that obtained from the synthesized map. From these measurements it seems that the flux scale varies by less than 5% over the region mapped.

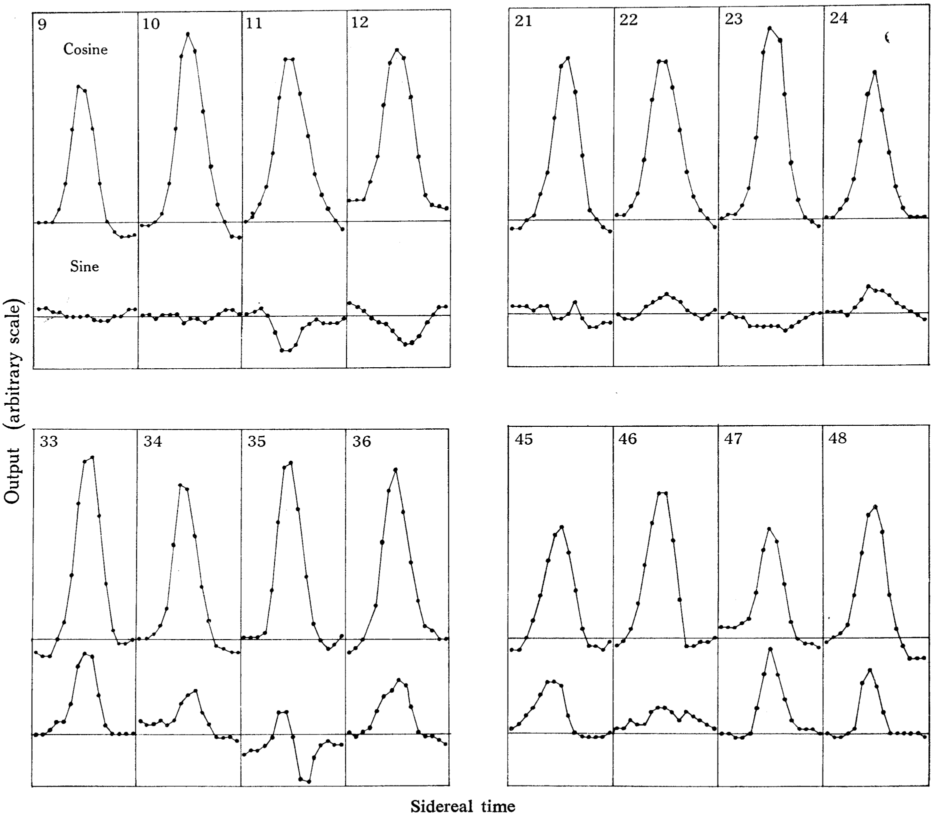

Fig. 2.—Cosine (upper) and sine (lower) components of the output produced by Hydra A at the indicated spacings. The phases have been rotated so that, apart from refraction effects, the sine component should be zero.

(*d*) *Flux Densities*

The flux densities listed in Table 2 have been obtained by comparing the peak brightnesses of sources on the synthesized maps (corrected for foreshortening of the NS array of spacings) with that of Hydra A taken as 1510 f.u. The quoted errors allow a 7% error in this value, a 4% error in the gain as a function of zenith angle, and an individually estimated error in the peak brightness determined for each source.

V. Spectra

The measurement of flux densities at 29·9 MHz allows improved values of spectral index to be derived for sources with a power law spectrum and also allows the recognition of certain sources with spectra which are curved at low frequencies.

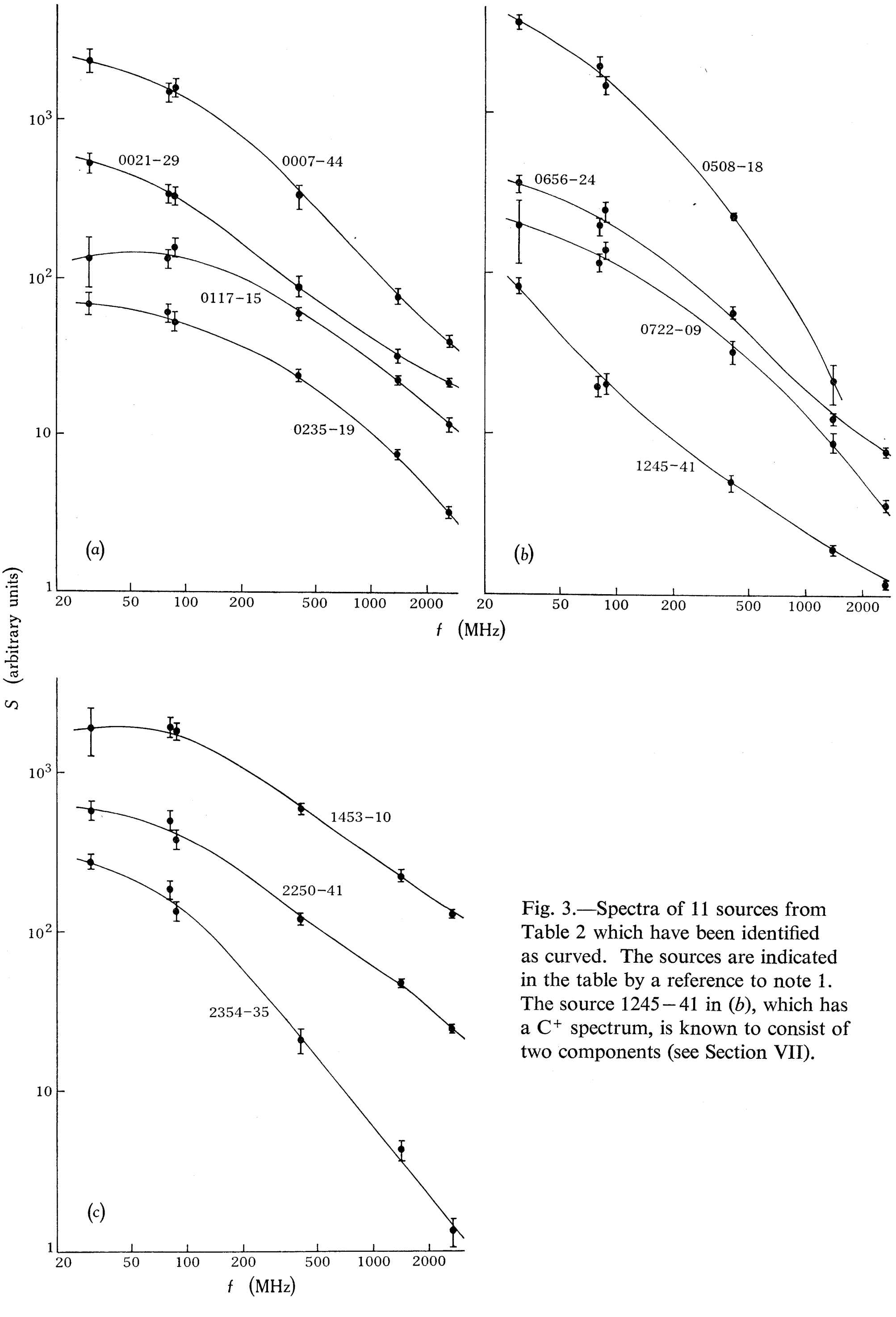

Fig. 3.—Spectra of 11 sources from Table 2 which have been identified as curved. The sources are indicated in the table by a reference to note 1. The source 1245−41 in (*b*), which has a C^+ spectrum, is known to consist of two components (see Section VII).

Straight line spectra of the form $\log S = \alpha \log f + \text{const.}$ have been fitted to the flux densities S at frequencies f of 29·9, 80, 85·5, 408, and 1410 MHz where these were available, using a least squares process. The higher frequency fluxes have been taken from the Culgoora survey (Slee and Higgins 1973), the MSH survey (Mills *et al.* 1958, 1960, 1961), and the Parkes catalogue (Bolton *et al.* 1964; Price and Milne 1965; Shimmins *et al.* 1966). The 85·5 MHz fluxes given in the MSH survey were reduced by a factor of 0·84 to bring the values to the CKL scale (Howard *et al.* 1965). The 408 and 1410 MHz values were taken from the original Parkes catalogue rather than the combined Parkes catalogue (Ekers 1969) since the former were based directly on measurements at the two frequencies and Wyllie (1969*b*) reports excellent agreement between the 408 MHz catalogue fluxes and absolute flux measurements made by him over each declination zone. The least squares fitting process was weighted in accordance with the quoted errors of each catalogue. A measure of the goodness of fit of the straight line spectrum to the points, namely the r.m.s. deviation of the points from the line in units of the standard error, was derived. On the basis of this measure it was decided whether a straight line spectrum adequately fitted the data. If the r.m.s. deviation from the line exceeded 0·8 standard errors, the source spectrum was plotted and if a regular curvature was apparent the spectrum was classed as curved. Figure 3 shows plots of curved spectra for 11 sources.

VI. Source List

An explanation of Table 2 is given below:

Column 1. The source number is the Parkes catalogue number (Ekers 1969) when appropriate or, failing this, the Culgoora-1 list number (Slee and Higgins 1973). When no such identification can be made, the number is determined from the 29·9 MHz position according to the same scheme.

Columns 2 and 3. The 29·9 MHz flux density and estimated error in flux units are given. A value in parentheses indicates the integrated flux density of an extended source.

Column 4. The MSH catalogue number (Mills *et al.* 1958, 1960, 1961) is given for sources which can be identified with an MSH source.

Column 5. C or P denotes that the source is listed in the Culgoora (Slee and Higgins 1973) or Parkes (Ekers 1969) catalogues.

Column 6. The spectral index α is that determined from the present 29·9 MHz flux densities (column 2) and those given in the Culgoora, MSH, and Parkes (generally excluding 2650 MHz values) catalogues. If a source was stated to be resolved but only its peak flux density was given, this value has been omitted from the calculation.

Column 7. The flux density at 100 MHz as determined by the line of best fit to the spectrum is given.

Column 8. The notation used to describe the spectrum relative to a power law with spectral index as given in column 6 is: S, no evidence of deviation from power law spectrum; C^+ or C^-, curved spectrum with low frequency radiation greater or less than that for power law; U, uncertain spectrum with poor fit to power law but no evident trend; R, spectrum unreliable because source is resolved at some frequencies.

TABLE 2

29·9 MHz FLUX DENSITIES AND SOURCE SPECTRA

(1) Source number	(2) $S_{29.9}$ (f.u.)	(3) $\Delta S_{29.9}$ (f.u.)	(4) MSH No.	(5) Other catalogues	(6) α	(7) S_{100} (f.u.)	(8) Spectrum	(9) Remarks*
0003−56	40	12	00−*51*	P	−0·77	15·0	S	III
0007−44	38	6	00−*43*	C, P	−0·74	18·3	C⁻	IIIB, note 1
0012−38	52	7	00−*33*	P	−0·97	15·6	S	III
0021−29	42	6	00−*25*	C, P	−0·70	21·3	C⁻	QSO, note 1
0023−33	37	6	00−*38*	C, P	−0·76	14·6	S	E gal
0035−39	31	12	00−*313*	C, P	−0·79	16·2	(C⁻)	III
0038−09	116	10	00−*011*	C, P	−1·03	33·1	U	
0043−42	63	12	00−*411*	C, P	−0·55	40·0	S	E gal
0045−25	32	11	00−*222*	C, P	−0·36	21·1	S	S gal
0100−22	59	12	01−*21*	C, P	−0·67	26·0	S	
0103−45	48	12	01−*41*	C, P	−0·88	25·6	(C⁻)	
0105−16	55	12	01−*12*	C, P	−0·62	34·5	S	III, 3C 32, spectrum may be curved above 1400 MHz
0112−32	31	6	01−*36*	P	−0·75	12·7	S	Parkes flux listed at 2650 MHz only
0114−47	43	7	01−*45*	C, P	−0·62	22·0	S	E gal
0117−15	33	12	01−*19*	C, P	−0·49	28·9	C⁻	III, 3C 38, note 1
0129−07	41	12	01−*06*		−0·91	13·8		IIIB
0130−62	83	13		P	−1·26	18·0	S	
0131−36	84	8	01−*311*	C, P	−0·70	39·1	S	S gal
0135−09	35	17	01−*08*		−0·80	13·3		
0148−29	54	7	01−*217*	C, P	−0·29	38·4	R	III, confused by PKS 0149−29
0157−31	52	7	01−*315*	C, P	−0·73	23·8	S	QSO
0207−42	32	12	02−*42*		−0·83	11·8		
0213−13	90	13	02−*15*	C, P	−0·89	30·7		Blend of PKS 0213−13·2 and 0213−13·5
0214−48	54	7	02−*43*	C, P	−0·73	21·6	S	May be slightly resolved
0216−36	52	12	02−*33*	C, P	−0·80	17·6	C⁻	III, spectrum curved above 400 MHz
0235−19	46	7	02−*110*	C, P	−0·41	32·3	C⁻	IIIB, note 1
0241−51	59	12	02−*53*	P	−0·69	26·7	S	
0245−55	101	9	02−*54*	P	−0·87	35·4	S	
0248−60	47	11	02−*64*		−1·03	13·6		
0253−23	38	6	02−*219*	C, P	−0·70	20·5	C⁻	III
0320−37	1840 (2120)	129	03−*31*	P	−0·82	667·1	S	S gal, Fornax A, slightly resolved
0336−35	52	12	03−*33*	C, P	−0·75	18·2	S	III
0349−14	111	10	03−*19*	C, P	−0·83	39·7	S	QSO
0349−27	116	10	03−*212*	C, P	−0·82	41·6	S	E gal
0350−07	47	17	03−*06*	C, P	−0·62	26·6	C⁻	QSO, 3C 94, spectrum curved above 400 MHz

0405 − 12	56	7	04 − *12*	C, P	−0·64	24·2	S	QSO
0411 − 34	31	6	04 − *33*	P	−0·81	11·7	S	III
0420 − 62	37	17	04 − *63*	P	−0·76	24·4	(C^-)	
0427 − 36	52	12	04 − *36*	C, P	−0·87	23·0	S	IIIB
0427 − 53	64	12	04 − *54*	P	−0·66	32·7	S	D gal
0429 − 61	36	17	04 − *64*	P	−0·88	21·6	(C^-)	
0442 − 28	121	10	04 − *218*	C, P	−0·72	53·7	S	E gal
0443 − 59	35	11		P	−0·91	11·7		
0486 − 20	37	6	04 − *219*	P	−0·85	12·6	S	E gal
0453 − 30	74	6	04 − *314*	C, P	−0·68	32·5		
0454 − 22	32	8	04 − *221*	C, P	−0·82	12·7	S	QSO
0502 − 10	34	12	05 − *11*	C, P	−0·74	15·6	S	D gal
0502 − 41	42	12						$05^h 02^m·7$, −41° 46′ [± 6′]
0503 − 28	63	12	05 − *22*	C, P	−1·01	30·4	U	III
0508 − 18	87	8	05 − *13*	C, P	−1·00	28·8	C^-	QSO, note 1
0511 − 48	87	18	05 − *42*	P	−0·77	32·7	S	
0518 − 45	958	67	05 − *46*	C, P	−0·73	395·2	S	E gal, Pictor A
0521 − 36	126	14	05 − *36*	C, P	−0·53	66·3	S	N gal
0600 − 34	63	7	06 − *31*	P	−1·16	15·4	R	III, blend of PKS 0600 − 34 and 0601 − 34
0600 − 39	53	7	05 − *319*		−1·10	14·1		
0612 − 47	43	6	06 − *43*	C, P	−0·85	12·7	S	
0614 − 39	32	6	06 − *35*		−1·49	5·3		
0616 − 48	38	6	06 − *44*	P	−1·04	10·2	S	
0618 − 37	42	6	06 − *37*	C, P	−0·76	15·4	S	D gal
0620 − 52	77	8	06 − *53*	P	−0·88	26·1	S	
0624 − 05	131	15	06 − *04*	C, P	−0·32	89·0	C^-	III, 3C 161, spectrum straight below 400 MHz
0625 − 54	290	21	06 − *55*	P	−1·06	80·4		
0625 − 35	42	6	06 − *38*	C, P	−0·65	21·7	S	D gal
0634 − 20	152	12	06 − *210*	C, P	−0·64	66·8	R	Blend of PKS 0634 − 20·4 and 0634 − 20·6
0646 − 39	48	7	06 − *312*	C, P	−0·79	18·7		III
0656 − 24	75	8	06 − *216*	C, P	−0·73	33·6	C^-	IIIA, note 1
0703 − 45	38	6	07 − *42*	C, P	−0·91	13·9	(C^-)	III, Culgoora source resolved
0705 − 07	47	7		P	−0·91	15·6		
0709 − 20	46	7	07 − *23*	C, P	−0·66	22·3	S	III
0715 − 25	32	12	07 − *24*	C, P	−0·62	19·4	(S)	IIIA
0719 − 55	44	12	07 − *53*	P	−0·84	16·8	S	III
0722 − 09	41	17	07 − *04*	C, P	−0·83	21·1	C^-	S gal, 3C 178, note 1
0723 − 06	48	17	07 − *05*		−0·16	38·4		May be slightly resolved
0736 − 38	32	6	07 − *312*	C	−0·41	19·8		
0738 − 25	40	6						$07^h 38^m·9$, −25° 02′ [± 6′]
0745 − 19	76	8	07 − *117*	C, P	−0·77	32·7	S	IIIA, possibly confused by PKS 0745 − 18

* See notes at end of table.

TABLE 2 (*Continued*)

(1) Source number	(2) $S_{29.9}$ (f.u.)	(3) $\Delta S_{29.9}$ (f.u.)	(4) MSH No.	(5) Other catalogues	(6) α	(7) S_{100} (f.u.)	(8) Spectrum	(9) Remarks*
0800 − 14	67	12	08 − *11*		− 1·42	12·1		
0806 − 10	80	8	08 − *14*	C, P	− 0·63	35·8	S	E gal
0807 − 38	53	18	08 − *31*	C, P	− 0·69	18·7	S	IIIA
0819 − 30	52	7	08 − *33*	C, P	− 0·85	20·4	U	E gal
0821 − 43	837 (1050)	60	08 − *44*		− 0·54	510	S	SNR, Puppis A, note 3
0847 − 57	69	8	08 − *53*	P	− 0·85	24·3	S	
0850 − 20	43	12	08 − *216*	C, P	− 0·78	18·2	S	III
0859 − 25	64	7	08 − *219*	C, P	− 0·61	35·6	(C^-)	III
0902 − 38	42	17	09 − 32	P	− 0·30	23·1	S	SNR
0915 − 11	1512	81	09 − *14*	C, P	− 0·90	513·5	S	D gal, Hydra A, 3C218, flux standard
0939 − 39	30	12	09 − *36*		− 1·44	5·4		
0942 − 54	46	7						$09^h 42^m{\cdot}5$, $-54° 03'$ [± 6′]
1002 − 21	97	9	10 − *21*	C, P	− 1·02	28·8	S	III
1005 − 56	89 (200)	9	10 − *51*					Possibly background irregularity
1017 − 42	96	9	10 − *44*	C, P	− 0·76		R	III, confused by PKS 1018 − 42
1017 − 58	69	8	10 − *53*		− 0·37	54	(C^-)	SNR, G284·2 − 1·8, absorption probable below 85 MHz, note 4
1045 − 19	32	12	10 − *120*	P	− 0·67	16·4	(S)	QSO, confused by PKS 1045 − 18
1045 − 59	81	8						$10^h 45^m{\cdot}2$, $-59° 23'$ [± 6′]
1053 − 27	42	12	10 − *216*		− 1·29	8·9		
1100 − 60	35	12	11 − *61*		− 0·59	225	C^-	SNR, G290·1 − 0·8, note 2
1122 − 59	55	9	11 − *54*		− 0·38	33·5	S	SNR, G292·0 + 1·8, note 5
1127 − 28	31	6	11 − *25*		− 0·64	14·4		
1131 − 17	33	11	11 − *17*	C, P	− 0·68	13·1	U	QSO, confused by PKS 1133 − 17
1136 − 13	45	17	11 − *18*	C, P	− 0·53	30·6	S	QSO
1138 − 26	42	12	11 − *27*	P	− 0·98	16·2	U	III
1139 − 28	52	12	11 − *28*	P	− 0·78	20·4	S	III
1146 − 11	34	12	11 − *113*	P	− 0·75	13·3	S	E gal
1149 − 54	45	12	11 − *56*		− 1·15	11·2		
1209 − 52	222	16	12 − *51*	P	− 0·80	84·5	R(S)	SNR, G296·3 + 10·0, PKS 1209 − 51 and 1209 − 52
1216 − 10	46	12	12 − *19*	C, P	− 0·63	20·4	S	III
1217 − 63	61	18	12 − *63*		− 0·84	22·1		
1233 − 24	48	7	12 − *27*	P	− 0·83	18·1	S	QSO
1236 − 55	45	7	12 − *53*		− 1·15	11·2		
1245 − 41	159	13	12 − *45*	C, P	− 1·14	36·8	R	Possibly blend of PKS 1245 − 41 and 1247 − 40, note 1
1251 − 28	42	12	12 − *212*	C	− 0·17	33·8		
1252 − 12	124	10	12 − *118*	C, P	− 0·70	49·0	C^+	D gal

1254−30	42	11	12−*38*	P	−0·99	16·1	S	
1333−33	157	12	13−*33*	P	−0·94	50·8		Blend of PKS 1332−33, 1333−33, and 1334−33
1343−60	1684	118	13−*62*		−0·72	605	S	SNR?, 13S6A, compare flux in Table 1, note 5
1345−25	117	10	13−*27*		−2·00	10·4		
1400−33	121	10	14−*32*	C, P	−1·00	36·9	S	E gal, resolved by Culgoora and Parkes at 1410 MHz
1416−15	44	7	14−*14*	C, P	−0·79	11·8	S	gal
1425−47	54	7	14−*46*		−0·76	21·6		
1427−50	44	12	14−*56*	P	−0·80	14·6	S	III
1437−59	80	30	14−*57*		−0·58	91·0	C^-	SNR, G316·3+0·0, note 2
1451−36	52	7	14−*38*	C, P	−0·65	25·7	S	QSO
1453−10	36	12	14−*121*	C, P	−0·63	29·2	C^-	QSO, note 1
1459−41	150	12	14−*415*	P	−0·89	49·6	U	SNR, G327·6+14·51
1508−25	37	12	15−*25*		−1·75	4·5		
1526−42	175	14	15−*43*	C	−0·80	66·6		
1548−56	371	42	15−*56*		−0·29	235·0	S	SNR, G326·2−1·7, note 6
1556−21	53	12	15−*213*	C, P	−0·76	20·7	S	III
1610−60	3192	220	16−*61*	P	−1·10	847·3	S	E gal, 16S6A, compare flux in Table 1
1622−31	53	7	16−*36*	C, P	−1·03	14·2	S	QSO?
1643−22	46	12	16−*29*	C, P	−0·69	15·7	S	IV
1710−24	215	16	17−*25*	C	−1·83	23·5		
1727−21	276	20	17−*211*	C, P	−1·08	74·9	S	SNR, G4·5+6·8, Kepler's supernova of 1604, note 7
1758−23	157	16	17−*216*		−0·45	800	C^-	SNR, G6·5−0·1, note 2
1817−39	42	17	18−*33*	C	−0·24	30·8		
1819−32	64	12						$18^h\,19^m·6$, −32° 53′ [±6′]
1834−43	53	7		P	−1·01	15·7	S	III
1840−40	53	7	18−*44*	C, P	−0·83	19·9	S	IIIA
1859−23	43	12	18−*21*	C, P	−0·64	25·2	S	IIIA
1912−26	80	8	19−*23*	C	−0·79	30·5	U	
1928−26	159	13	19−*28*	C	−1·72	19·9	U	
1932−11	68	19	19−*110*		−0·85	25·1		
1932−46	215	16	19−*46*	C, P	−0·73	97·4	(C^-)	
1940−40	64	7	19−*410*	C, P	−0·98	20·0	S	III
1941−07	47	12	19−*011*	P	−0·71	19·1	S	III
2030−23	32	12	20−*28*	C, P	−0·54	14·5	S	D gal
2032−35	47	17	20−*37*	C, P	−0·70	30·4	S	III
2041−60	82	18	20−*61*	P	−0·88	34·2	S	III
2048−57	91	18	20−*57*	P	−1·09	24·5	U	S gal
2058−28	137	11	20−*215*	C, P	−0·88	44·0	(S)	E gal
2104−25	180	14	21−*21*	C, P	−0·73	74·4	S	E gal
2105−05	70	12	21−*04*		−1·51	11·3		
2120−16	55	7	21−*19*	C, P	−0·65	24·6	(S)	III, blended with PKS 2119−16

* See notes at end of table.

TABLE 2 (*Continued*)

(1) Source number	(2) $S_{29\cdot9}$ (f.u.)	(3) $\Delta S_{29\cdot9}$ (f.u.)	(4) MSH No.	(5) Other catalogues	(6) α	(7) S_{100} (f.u.)	(8) Spectrum	(9) Remarks*
2122−55	40	12						$21^h 22^m\cdot4$, $-55° 32'$ [±6′]
2124−12	51	7	*21−111*	P	−0·85	17·1	(C^+)	
2135−14	67	7	*21−115*	C, P	−0·68	28·0	S	QSO
2141−56	51	11	*21−56*		−1·15	12·6		
2154−18	33	17	*21−123*	C, P	−0·47	19·1	S	QSO
2211−17	296	22	*22−17*	C, P	−0·82	107·8	S	D gal
2218−50	39	6	*22−51*	P	−0·75	14·8	S	III
2223−52	44	12	*22−52*	P	−0·75	20·0	S	
2250−41	52	7	*22−43*	C, P	−0·63	29·6	C^-	III, note 1
2313−62	54	12	*23−64*		−1·46	9·4		
2317−27	42	6	*23−24*	C, P	−0·64	18·7	S	E gal
2317−22	28	12	*23−25*	P	−0·88	9·5		
2322−05	41	12	*23−010*	C, P	−0·83	15·8	S	N gal, blended with PKS 2325−05
2322−12	34	6	*23−112*	C, P	−0·55	20·5	S	E gal
2331−41	69	8	*23−44*	C, P	−0·64	35·3	(C^-)	III
2334−35	37	6	*23−34*	P	−0·85	14·3	S	III
2338−58	52	18	*23−52*	P	−0·79	19·2	S	
2345−28	42	6	*23−211*		−1·15	10·5		
2347−25	32	6	*23−213*		−0·83	11·8		
2354−35	68	7	*23−37*	C, P	−0·92	26·6	C^-	D gal, note 1
2356−61	403	29	*23−64*	P	−0·75	173·7	U	D gal
2359−36	37	6	*23−38*		−0·85	13·2		

* Notes:

1. Spectrum is plotted in Figure 3.
2. Source is an SNR with curved spectrum at low frequency. The values of α and S_{100} are based on high frequency measurements. See Figure 4.
3. Spectrum is based on measurements at 29·9 MHz (present results), 85·5 MHz (MSH), and 635, 1410, and 2650 MHz (Milne and Hill 1969).
4. Spectrum is based on measurements at 29·9 MHz (present results), 85·5 MHz (MSH), and 1400 and 2700 MHz (Milne 1972).
5. Spectrum is based on measurements at 29·9 MHz (present results), 85·5 MHz (MSH), 408 MHz (Shaver and Goss 1970), and 5000 MHz (Goss and Shaver 1970).
6. Spectrum is based on measurements at 29·9 MHz (present results), 85·5 MHz (MSH), 408 MHz (Komesaroff 1966), and 1410 and 2650 MHz (Manchester 1969).
7. Spectrum calculation uses Parkes 2650 MHz flux density.

Column 9. Information relating to optical identifications, the measured 29·9 MHz positions of uncatalogued sources, and references to notes appended to the table are given. The optical identifications are taken from the Parkes and Culgoora catalogues and from Milne (1969) for some supernova remnants (SNR's). The symbols III, IIIA, IIIB, and IV refer to optical fields where no identifications have been made, their use being the same as in the Parkes and Culgoora catalogues.

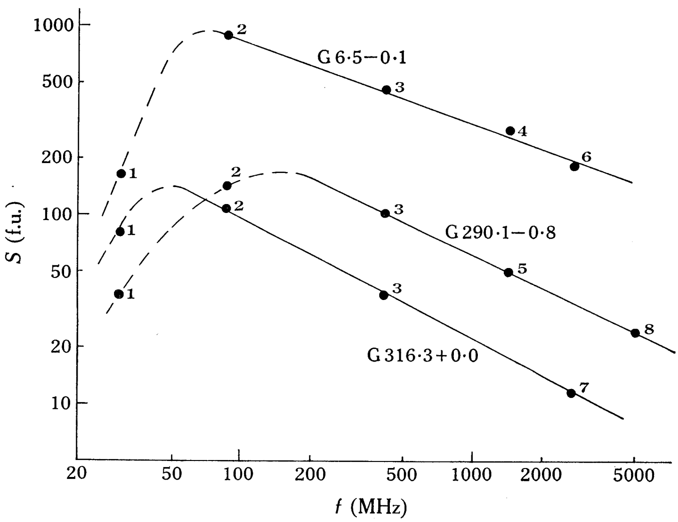

Fig. 4.—Spectra of SNR's at low galactic latitudes for which the reduced value of $S_{29.9}$ is attributed to absorption by the interstellar medium. The indicated references to flux density data are: 1, present results; 2, Mills *et al.* (1961) at 85·5 MHz; 3, Shaver and Goss (1970) at 408 MHz; 4, Milne and Hill (1969) at 1410 MHz; 5, Manchester (1969) at 1410 MHz; 6, Milne and Hill (1969) at 2650 MHz; 7, Day *et al.* (1969) at 2650 MHz; 8, Milne (1969) at 5000 MHz.

VII. Discussion

Of the 134 sources for which spectra were fitted to three or more points, only 18 are definitely identified as having curved spectra. Three with reduced flux densities at low frequencies (C^- spectra) are SNR's at low galactic latitudes and their reduced flux densities at 29·9 MHz probably result from absorption by the interstellar medium. The spectra of these sources are shown in Figure 4.

A check was made to find which sources listed in the MSH catalogue as having flux densities above 40 f.u. at 85·5 MHz were not detectable on the synthesized maps. Most of these undetected sources are thermal but 12 could be identified from the high frequency measurements as having nonthermal spectra. However, all of these nonthermal sources have galactic latitudes of less than 3°, which supports the suggestion that the reduced flux density at low frequencies is caused by interstellar absorption. (The authors are currently preparing a paper in which absorption near the galactic plane is considered in more detail.) At higher galactic latitudes, curvatures of spectra are presumably inherent to the sources.

Only one source (1252−12) definitely showed a C^+ spectrum. This may be a composite source with two nonthermal components of different spectral indices. The source 1245−41 (the spectrum of which is given in Fig. 3(*b*)) has a C^+ spectrum, but this definitely consists of two components as shown by the high resolution surveys. QSO's were represented disproportionately among the sources with C^- spectra, 4 of the 15 QSO's listed showing definite curvature in their spectra. Optical identifications are unavailable for all but two (0722−09, an S galaxy, and 2354−35, a D galaxy) of the remaining sources with C^- spectra.

VIII. Acknowledgments

The authors wish to thank Mr. A. C. O. Gibb who took part in the development of the EW array and Mr. R. H. Mondel who designed the feed system for it. One of us (B.B.J.) acknowledges the assistance of a Commonwealth Postgraduate Studentship.

IX. References

Bolton, J. G., Gardner, F. F., and Mackey, M. B. (1964).—*Aust. J. Phys.* **17**, 340.
Conway, R. G., Kellermann, K. I., and Long, R. J. (1963).—*Mon. Not. R. astr. Soc.* **125**, 261.
Day, G. A., Thomas, B. M., and Goss, W. M. (1969).—*Aust. J. Phys. astrophys. Suppl.* No. 11, 11.
Ekers, Jennifer A. (Ed.) (1969).—*Aust. J. Phys. astrophys. Suppl.* No. 7.
Finlay, E. A., and Jones, B. B. (1972).—*Proc. astr. Soc. Aust.* **2**, 115.
Goss, W. M., and Shaver, P. A. (1970).—*Aust. J. Phys. astrophys. Suppl.* No. 14, 1.
Howard, W. E., Dennis, T. R., Maran, S. P., and Aller, H. D. (1965).—*Astrophys. J. Suppl. Ser.* **10**, 331.
Kellermann, K. I., Pauliny-toth, I. I. K., and Williams, P. J. S. (1969).—*Astrophys. J.* **157**, 1.
Komesaroff, M. M. (1966).—*Aust. J. Phys.* **19**, 75.
Little, A. G. (1958).—*Aust. J. Phys.* **11**, 70.
Manchester, Barbara A. (1969).—*Aust. J. Phys. astrophys. Suppl.* No. 12.
Mills, B. Y., Slee, O. B., and Hill, E. R. (1958).—*Aust. J. Phys.* **11**, 360.
Mills, B. Y., Slee, O. B., and Hill, E. R. (1960).—*Aust. J. Phys.* **13**, 676.
Mills, B. Y., Slee, O. B., and Hill, E. R. (1961).—*Aust. J. Phys.* **14**, 497.
Milne, D. K. (1969).—*Aust. J. Phys.* **22**, 613.
Milne, D. K. (1972).—*Aust. J. Phys.* **25**, 307.
Milne, D. K., and Hill, E. R. (1969).—*Aust. J. Phys.* **22**, 216.
Price, R. M., and Milne, D. K. (1965).—*Aust. J. Phys.* **18**, 329.
Shain, C. A., Komesaroff, M. M., and Higgins, C. S. (1961).—*Aust. J. Phys.* **14**, 508.
Shaver, P. A., and Goss, W. M. (1970).—*Aust. J. Phys. astrophys. Suppl.* No. 14, 77.
Shimmins, A. J., Day, G. A., Ekers, R. D., and Cole, D. J. (1966).—*Aust. J. Phys.* **19**, 837.
Slee, O. B., and Higgins, C. S. (1973).—*Aust. J. Phys. astrophys. Suppl.* No. 27.
Williams, P. J. S., Kenderdine, S., and Baldwin, J. E. (1966).—*Mem. R. astr. Soc.* **70**, 53.
Wyllie, D. V. (1969*a*).—*Mon. Not. R. astr. Soc.* **142**, 229.
Wyllie, D. V. (1969*b*).—*Proc. astr. Soc. Aust.* **1**, 234.